JURNAL NATURAL

Vol. 24, (1) 2024
DOI 10.24815/jn.v24i1.33247

pISSN 1411-8513
eISSN 2541-4062

ORIGINAL RESEARCH

On the dynamics of spring-pendulum system: an overview of configuration space and phase space

SITI WAHYUNI[1*], NUR WIDYA RINI[2], JOKO SAEFAN[2]

[1]Department of Physics, Universitas Negeri Semarang, Semarang, Indonesia
[2]Department of Physics Education, Universitas PGRI Semarang, Semarang, Indonesia

*Corresponding Author: wahyuni.smg@mail.unnes.ac.id

Received: 23 July 2023
Revised: 11 December 2023
Accepted: 16 January 2024

Abstract. The dynamics of the spring-pendulum system with two degrees of freedom were studied. The motion of this system is restricted to be in a vertical plane so that the chosen generalized coordinates are the increased length of the spring u and the swing angle of pendulum θ. Hamiltonian of the system is obtained from the Legendre transformation of Lagrangian. Hamilton's equation yields four differential equations that represent the dynamic of the system. The obtained results were visualized in configuration space and phase space trajectories. It is shown that generally the greater the initial swing angle, the more complex pattern will occur followed by the appearance of chaotic phenomena.

Keywords: spring-pendulum, Hamilton's equation, configuration space, phase space, chaotic phenomenon.

INTRODUCTION

The review of the physical pendulum system is still evolving even though it is a very familiar case in classical mechanics. One of them is a physical pendulum system driven by a magnetic field through a theoretical and numerical analysis of one-side oscillation [1]. The existence of chaotic behavior and multiperiodicity for various values of the frequency of the current signal was shown from bifurcation diagrams obtained numerically and verified by experimental estimates. Previously, observations of magnetic interactions in the double pendulum system had been carried out numerically and experimentally [2]. Few chaotic zones have been detected numerically and confirmed experimentally, where the bifurcation diagrams are also used to show the scenarios of transition from regular to chaotic motion and vice versa. The chaotic motions of a double pendulum demonstrate how complicated the motion of a simple dynamic system can be when the system and the motion become nonlinear [3-6]. The next work is a double pendulum case that has been modeled with the fractional dynamics approach to find their equation of motion [7]. Moreover, a double pendulum system with magnetic field interaction has been adopted to improve the efficiency of piezoelectric energy harvesters (PEH) to harvest energy from human motions [8].

Apart from the double pendulum, the case that is often discussed is the spring-pendulum system. Wahyuni et al. have derived the equations of motion for this case in their Lagrangian form [9]. The equation of motion represented by the second-order differential equation is obtained from the two general coordinates used, i.e. the increase in the length of the spring and the angle of the pendulum. The same system but with a different arrangement was studied by Rini *et al.,* namely by inverting the spring to be at the bottom of the pendulum [10]. Both of these systems are solved by the Lagrangian method, and then the dynamics of the generalized coordinates to time are described. In addition, the usual way of describing system dynamics can be done through configuration space and phase space. Configuration space is the space defined by the generalized coordinates, while phase space is defined by the position and momentum of the particle as they change in time. The state of a particle can be represented by a point in phase space, and its movement consequently creates a path or trajectory within that space [11].

This study is a continuation of the work of Wahyuni *et al*. [9] with a Hamiltonian review. The work only derives the Lagrangian equation and then describes the generalized coordinate dynamics of u and θ with respect to time. This study is very different from the studies mentioned above [1-11] because this is only a theoretical study. The important point of this study is the process of deriving the system's equations of motion and then visualizing it from different spaces, namely the configuration space and the phase space. This drawing will be carried out for several samples of initial swing angles.

METHODOLOGY

The Spring-Pendulum System

The spring-pendulum system was depicted in Figure 1, consisted of the spring with length l_1, increased length of the spring u, and mass m_1 in the end of spring. In addition, the pendulum with mass m_2 connected to the mass m_1 with the massless rod l_2. The angle θ represent the swing angle of the pendulum with respect to the vertical line. We assume that all movement occurs in two dimensionals, vertical plane. It is assumed that the spring can only move up and down in oscillations, not deviate with the pendulum, which represents applications in daily tools that springs only move in one dimension. The mass m_1 is constrained by the spring constant, and the pendulum is constrained by the constant length of the rod. Starting from two degrees of freedom for each of the two objects, the two constraints reduce the number of degrees of freedom to two, one for each object.

Research Methodology

Based on Figure 1 we can determine that the generalized coordinates for this system are u and θ. The Hamiltonian (H) of this system is given by the Legendre transformation of the Lagrangian (L) and Hamilton's equation of this system as two pairs of first-order differential, i.e. θ coordinates representation as

$$-\dot{p}_\theta = \frac{\partial H}{\partial \theta} \quad ; \quad \dot{\theta} = \frac{\partial H}{\partial p_\theta} \tag{1}$$

and u coordinates representation as

$$-\dot{p}_u = \frac{\partial H}{\partial u} \quad ; \quad \dot{u} = \frac{\partial H}{\partial p_u} \tag{2}$$

The study of such differential equations is crucial for understanding the system's behavior. These two pairs yield four equations of motion were solved using numerical methods. The numerical method chosen is the 4th order Runge-Kutta which has a good approximation [12-15]. Let $\frac{dy}{dx} = f(y,x)$, we can find the approximation of $y(x+\Delta x)$ as

$$y(x+\Delta x) = y(x) + \frac{1}{6}(j_1 + 2j_2 + 2j_3 + j_4) \tag{3}$$

where

$$j_1 = \Delta x\, f(y,x)$$
$$j_2 = \Delta x\, f\left(y + \frac{j_1}{2}, x + \frac{\Delta x}{2}\right)$$
$$j_3 = \Delta x\, f\left(y + \frac{j_2}{2}, x + \frac{\Delta x}{2}\right)$$
$$J_4 = \Delta x\, f(y + j_3, x + \Delta x)$$

We use the visualization results only to explain the dynamics of motion. So, the solution of the differential equations was not generated, but are presented in the form of graphs that represent the motion of objects, both in the configuration space and the phase space. To facilitate visualization, several parameters are used as needed.

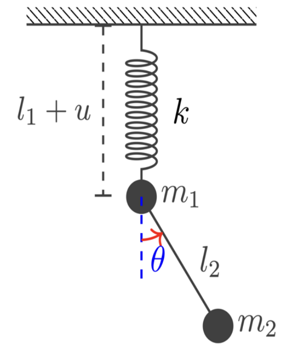

Figure 1. Spring-pendulum system

RESULTS AND DISCUSSION

The Hamilton's Equation

The Lagrangian of the system is given by the equation

$$L = \frac{1}{2}(m_1+m_2)\dot{u}^2 + \frac{1}{2}m_2\left(l_2{}^2\dot{\theta}^2 - 2l_2 \sin\theta\dot{\theta}\dot{u}\right) - \frac{1}{2}ku^2 + m_2 g(u + l_2\cos\theta) \tag{4}$$

where $\dot{u} = du/dt$ and $\dot{\theta} = d\theta/dt$ [9]. The Lagrangian was chosen where the zero potential energy at the point m_1 hanged.

The generalized momenta p_θ and p_u we obtain respectively as

$$p_\theta = \frac{\partial L}{\partial \dot{\theta}} = m_2 l_2{}^2\dot{\theta} - m_2 l_2 \sin\theta\dot{u} \tag{5}$$

$$p_u = \frac{\partial L}{\partial \dot{u}} = -m_2 l_2 \sin\theta\dot{\theta} + (m_1+m_2)\dot{u}. \tag{6}$$

Equation (5) multiply with $\sin\theta$ and equation (6) multiply with l_2 respectively yield

$$\sin\theta\ p_\theta = m_2 l_2{}^2 \sin\theta\dot{\theta} - m_2 l_2 \sin^2\theta\dot{u} \tag{7}$$

$$l_2 p_u = -m_2 l_2{}^2 \sin\theta\dot{\theta} + l_2(m_1+m_2)\dot{u}. \tag{8}$$

Eliminate $\dot{\theta}$ from equation (7) and (8) by adding them together, so we get

$$\sin\theta\ p_\theta + l_2 p_u = \left(l_2(m_1+m_2) - m_2 l_2 \sin^2\theta\right)\dot{u} \tag{9}$$

In the end, we obtain the rate of increased length of the spring with time as

$$\dot{u} = \frac{\sin\theta p_\theta + l_2 p_u}{l_2\left(m_1+m_2-m_2\sin^2\theta\right)} \tag{10}$$

To get the rate of swing angle with time, substitute equation (10) into equation (5), we get

$$p_\theta = m_2 l_2{}^2\dot{\theta} - m_2 l_2 \sin\theta\left(\frac{\sin\theta p_\theta + l_2 p_u}{l_2\left(m_1+m_2-m_2\sin^2\theta\right)}\right) \tag{11}$$

$$m_2 {l_2}^2 \dot{\theta} = \frac{(m_1 + m_2)\, p_\theta + m_2 l_2 \sin\theta p_u}{(m_1 + m_2 - m_2 \sin^2\theta)} \tag{12}$$

$$\dot{\theta} = \frac{(m_1 + m_2)\, p_\theta + m_2 l_2 \sin\theta p_u}{m_2 {l_2}^2 (m_1 + m_2 - m_2 \sin^2\theta)} \tag{13}$$

The Hamiltonian (H) of mechanical system in function of the rate of coordinates with time, conjugate momenta, and Lagrangian is obtain using Legendre Transformation, i.e

$$H = \textstyle\sum_i p_i \dot{q}_i - L. \tag{14}$$

with p_i is the generalized momenta and $\dot{q}_i = dq_i/dt$ where q_i is the generalized coordinates [16]. We obtain

$$H = p_u \dot{u} + p_\theta \dot{\theta} - L(u, \theta, \dot{u}, \dot{\theta}). \tag{15}$$

Substitute equations (4), (10), and (13) together into equation (15), we get Hamiltonian of the spring-pendulum system as

$$H = \frac{(m_1 + m_2){p_\theta}^2}{2 m_2 {l_2}^2 (m_1 + m_2 \cos^2\theta)} + \frac{{p_u}^2}{2(m_1 + m_2 \cos^2\theta)} + \frac{\sin\theta p_\theta p_u}{l_2 (m_1 + m_2 \cos^2\theta)} + \frac{1}{2} k u^2 - m_2 g (u + l_2 \cos\theta) \tag{16}$$

Decomposing equation (16) with the set of equations (1) and (2) yields four first-order differential equation, that are.

$$-\dot{p}_\theta = \frac{a m_2 (m {p_\theta}^2 + m_2 {l_2}^2 {p_u}^2)}{b} + \frac{a(b + c) p_\theta p_u}{l_2 b^2} + gc \tag{17}$$

$$-\dot{p}_u = ku - m_2 g \tag{18}$$

$$\dot{\theta} = \frac{m p_\theta}{b m_2 {l_2}^2} + \frac{c p_u}{b l_2 m_2} \tag{19}$$

$$\dot{u} = \frac{p_u}{b} + \frac{c p_\theta}{b l_2 m_2} \tag{20}$$

where $m = m_1 + m_2, a = 2 \sin\theta \cos\theta, b = m_1 + m_2 \cos^2\theta$, and $c = m_2 \sin\theta$.

Let $[\dot{p_\theta}, \dot{p_u}, \dot{\theta}, \dot{u}] = [x_1, x_2, x_3, x_4] = x_i$ where $i = 1, 2, 3$ and 4, and the solutions of equation (17-20) $[p_\theta, p_u, \theta, u] = [y_1, y_2, y_3, y_4] = y_i$. So the numerical solution as 4th order Runge-Kutta method can be written as

$$y_i(t + h) = y_i(t) + \frac{1}{6}(j_{i1} + 2j_{i2} + 2j_{i3} + j_{i4}) \tag{21}$$

Where $j_{i1} = h x_i(t, y_i)$, $j_{i2} = h x_i\left(t + \frac{h}{2}, y_i + \frac{j_{i1}}{2}\right)$, $j_{i3} = h x_i\left(t + \frac{h}{2}, y_i + \frac{j_{i2}}{2}\right)$, $j_{i4} = h x_i(t + h, y_i + j_{i3})$, and h is time step.

There are several representations to describe the equation of motion, such as time evolution, configuration space, phase-space, Poincare section, bifurcation, or the detailed methods to expose the motion. For example, Amer et al. uses evolutionary time, phase space, and Poincare representations to describe system dynamics [17]. In this work, we vary the initial swing angle θ_0 to visualize the configuration space and the three-dimensional phase space. The initial coordinates of the motion are (0,0,0) and the parameters used for all the visualization are shown in Table 1.

Table 1. Parameters used for all the visualization

Symbol	Description	Value	Unit
l_1	equilibrium spring length	1	m
l_2	rod length	1	m
m_1	mass attached at the spring	0.1	kg
m_2	mass attached at the rod	0.1	kg
g	gravitation constant	9.8	ms^{-2}
k	spring constant	10	Nm^{-1}

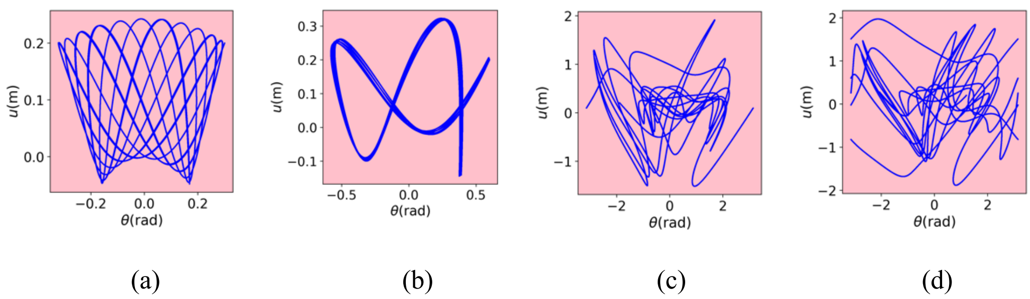

Figure 2. Configuration spaces for spring-pendulum with $u_0 = 0.2$ m, $p_{u_0} = p_{\theta_0} = 0$, and initial angle θ_0 (a) 0.3 rad, (b) 0.6 rad, (c) 0.9 rad, (d) 1.2 rad.

Figure 2 demonstrates the configuration space on the planes (θ, u) where several phase trajectories with constant initial value $u_0 = 0.2$ m, $p_{u_0} = p_{\theta_0} = 0$ and corresponding to different values θ_0. The plane area was $l_1 - u$ to $l_1 + u$ and $-\theta_0$ to $+\theta_0$. It can be seen that for small values θ_0 phase trajectories are corresponding to motion on the linear oscillation mode. These shapes gradually begin to distort with increasing θ_0 and turn into other phase trajectories that are more complex in character. This is same interpretation with the work of Smirnov *et.al.* [18].

The three-dimensional phase-space was shown in Figure 3. The system was plotted for initial values $u_0 = 0.2$ m, $p_u = p_\theta = 0$ and corresponding initial angles, $\theta_0 = 0.6$ rad and $\theta_0 = 1.2$ rad. Those values are chosen for the simulation to distinguish significant states of the system. The simulations have allowed the motion to evolve for a time $T = 15$ seconds with $\Delta T = 0.00001$. The vertical axis represents time evolution or the flow of the time, while the horizontal axes represent the two phase-space coordinates separately, (θ, p_θ) and (u, p_u). This description follows Semkiv *et al.* [19] who made an integral curve in the phase space. In this work, coordinates u represent the spring motion, while coordinates θ represent the pendulum motion. System leads to periodic motion for small angle $\theta_0 = 0.6$ rad, while for large angle $\theta_0 = 1.2$ rad indicates system approach to a chaotic motion.

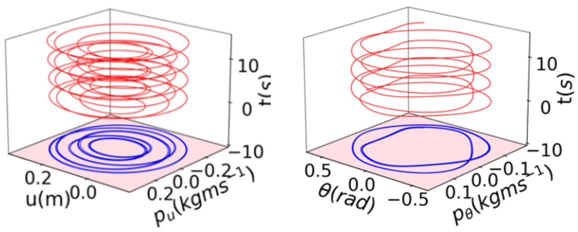

(a)

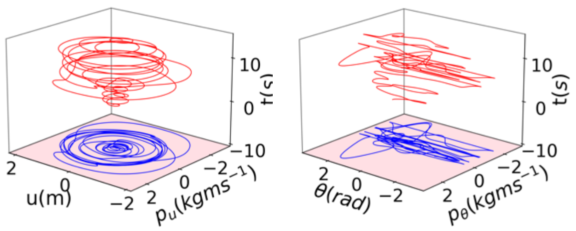

(b)

Figure 3. Three-dimensional phase space plot of motion the spring-pendulum system with initial values $u_0 = 0.2$ m, $p_u = p_\theta = 0$ and initial angles (a) $\theta_0 = 0.6$ rad, (b) $\theta_0 = 1.2$ rad.

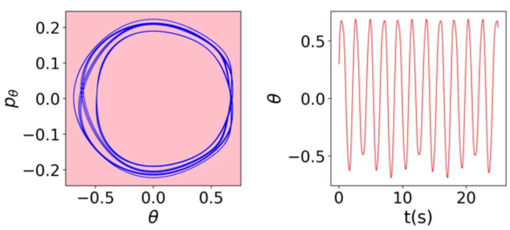

(a)

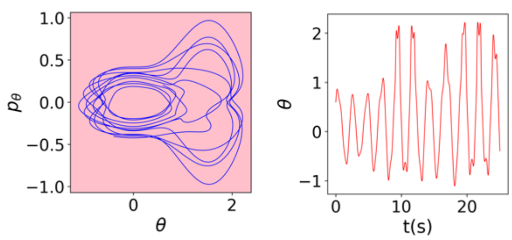

(b)

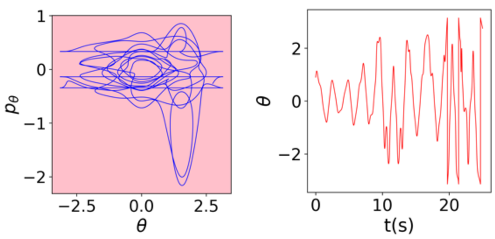

(c)

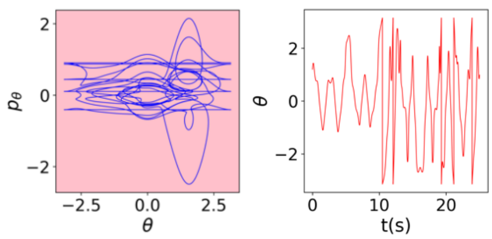

(d)

Figure 4. Phase-space plot of motion of the spring-pendulum system with initial values $u_0 = 0.2$ m, $p_{u_0} = 0, p_{\theta_0} = 0.2$ kg ms^{-1} and initial values θ_0 (a) 0.3 rad, (b) 0.6 rad, (c) 0.9 rad, (d) 1.2 rad.

Figure 3(a) shows that the dynamics of the system with small angle condition is predictable for both u and θ coordinates. However, a different situation can be seen in Figure 3(b), where u coordinates can still be predicted, but θ coordinates already show a chaotic phenomenon. It can be seen that even though the u coordinates appear irregular but there is no broken path, different from the θ coordinates. Therefore, it becomes interesting to investigate the θ coordinates further.

In order to investigate the characteristics of θ coordinates, we describe a two-dimensional phase space in the (θ, p_θ) plane compared to time evolution of θ. Each left side of Figure 4 shows a two-dimensional projection of a phase-space for the initial values $u_0 = 0.2$ m, $p_{u_0} = 0$, $p_{\theta_0} = 0.2$ kg ms^{-1} with different initial angles. The closed curve of Figure 4(a) and 4(b) is composed of eleven overlapping projected curves, in accordance with eleven patterns of oscillation in right side of the figure. Even though there are slight variations, it can still be said that system move in smooth oscillations. The precise alignment and closure of these curves demonstrate the stability and precise repetition of the oscillation. The presence of repeated oscillation patterns proves that small swing angles lead to steady state oscillations.

The greater the initial angle, more complex trajectories of the systems. It can be seen in Figures 4(c) and 4(d) that the horizontal scale has exceeded the range $-\pi \leq \theta \leq \pi$. Because it has exceeded one period 2π, the visualization starts again from -π so that several broken patterns appear. The chaotic phenomenon is strengthened by the increasingly irregular oscillation patterns that appear both in the visualization of the phase space and time evolution of θ. This allows us to visually illustrate one of the defining characteristics of a complex system: unpredictable behavior. The state space is high-dimensional making it difficult to analyze and visualize the behavior of the system for varying input conditions [20]. It turns out that theoretical studies like this can also be developed and applied in everyday life, for example controlling the kinematics of a spring-pendulum system using an energy harvesting device. This model has become essential in recent times as it uses control sensors in industrial applications, buildings, infrastructure, automobiles, and transportation [21].

CONCLUSION

The Hamiltonian of the spring-pendulum system has been derived with the general coordinates was the increase in the length of the spring u and the swing angle of the pendulum θ. Visualization results in configuration space and phase space trajectory show that in general the larger the initial swing angle, the more complex patterns will occur with complex characteristics, followed by the appearance of chaotic phenomena.

REFERENCE

[1] Wijata, A.; Polczynski, K.; and Awrejcewicz, J. 2021. Theoretical and numerical analysis of regular one-side oscillations in a single pendulum system driven by a magnetic field. *Mech. Sys. Sig. Proces.* **150**. DOI: 10.1016/j.ymssp.2020.107229.

[2] Wojna, M.; Wijata, A.; Wasilewski, G.; Awrejcewicz, J. 2018. Numerical and experimental study of a double physical pendulum with magnetic interaction. *J. Sound and Vibration.* **430**, 214-230. DOI: 10.1016/j.jsv.2018.05.032

[3] Zhou, Z; Whiteman, C. 1996. Motions of a Double Pendulum. *Nonlinear Anal. Theory, Meth. Appl.* **26** (7). 0362-546X(94)60253-3.

[4] Rega, G.; Settimi, V.; Lenci, S. 2020. Chaos in one-dimensional structural mechanics. *Nonlinear Dynamics* **102**, 785-834. DOI: 10.1007/s11071-020-05849-3.

[5] Avanço, R H.; Balthazar, J M.; Tusset, Â M.; Ribeiro, M A. 2021 Short comments on chaotic behavior of a double pendulum with two subharmonic frequencies and in the main resonance zone. ZAMM – *J. Appl. Math. Mech.* **101**(12). DOI: 10.1002/zamm.202000197

[6] Litak, G.; Borowiec, M.; Dąbek, K. 2022. The transition to chaos of pendulum systems. *Appl. Sci.* **12**(17) 8876. DOI: 10.3390/app12178876

[7] Anli, E; Ozkol, I. 2010. Classical and Fractional-Order Analysis of the Free and Forced Double Pendulum. *Eng.* **2**, 935-949. DOI:10.4236/eng.2010.212118

[8] Izadgoshasb, I; Lim, Y. Y.; Tang, L. Padilla, R. V.; Tang, Z. S.; Sedighi, M. 2019. Improving efficiency of piezoelectric based energy harvesting from human motions using double pendulum system. *J. En. Conver. Manag.* **184**, 559-570. DOI: 10.1016/j.enconman.2019.02.001

[9] Wahyuni, S.; Irawati, E.; and Saefan, J. 2022. Mekanika Pegas-Pendulum Tergandeng dalam Tinjauan Lagrangian. *Lontar Phys. Forum VI*, 37-42. ISSN 2963-2587.

[10] Rini, N.W.; Saefan, J.; Khoiri, N. 2023. Lagrangian Equation of Coupled Spring-Pendulum System. *Phys. Com.* **7** (1), 22-27. DOI: 10.15294/physcomm.v7i1.40771.

[11] Bhattacharya, T.; Habib, S.; Jacobs, K. 2002. The Emergence of the Classical Dynamics in Quantum World. *Los Alamos Sci.* **27** 110-125. DOI: 10.48550/arXiv.quant-ph/0407096

[12] Chauhan, V.; Srivastava, P,K. 2019. Computational Techniques Based on Runge-Kutta Method of Various Order and Type for Solving Differential Equations. *Int. J. Math. Eng. Manag. Sci.* **4** (2), 375–386. DOI: 10.33889/IJMEMS.2019.4.2-030

[13] Dang, Q A. & Hoang, M T. 2020. Positive and elementary stable explicit nonstandard Rune-Kutta methods for a class of autonomous dynamical systems. *Int. J. Comp. Math.* **97**(10), 2036-2054. DOI: 10.1080/00207160.2019.1677895

[14] Alcin, M. 2020. The Runge Kutta-4 based 4D Hyperchaotic System Design for Secure Communication Applications. *Chaos Theory and Appl.* **2**(1), 23-30.

[15] Ranocha, H. 2020. On strong stability of explicit Runge-Kutta methods for nonlinear semibounded operators. *IMA J. Num. Anal.* **41**(1), 654-682. DOI 10.1093/imanum/drz070

[16] Mann, P. 2018 *Lagrangian and Hamiltonian Dynamics*. Oxford University Press. DOI: 10.1093/oso/9780198822370.001.0001

[17] Amer, T.S.; Galal, A.A.; Abolila, A.F. 2021. On the motion of a triple pendulum system under the influence of excitation force and torque. *Kuwait J. Sci.* **48** (4), 1-17. DOI: 10.48129/kjs.v48i4.9915

[18] Smirnov, A.S.; Smolnikov, B.A. 2021. Nonlinear oscillation modes of double pendulum. *IOP Conf. Ser.: Mat. Sci. Eng.* DOI10.1088/1757-899X/1129/1/012042.

[19] Semkiv, O.M.; Shevchenko, S.M.; Slepuzhnikov, E.D. 2022 *Geometrical modeling of the resonance of an oscillating spring depending from its parameters*. Ukraine: Publisher Oleksandr Mykolayovych Tretyakov. ISBN 978-617-7827-34-3.

[20] Bartolovic, N.; Gross, M.; Gunther, T. 2020 Phase Space Projection of Dynamical Systems. *Eurographics Conf. Visualization (EuroVis)*. **39** (3), 253-264. DOI: 10.1111/cgf.13978

[21] He, CH.; Amer, T.S.; Tian, D.; Abolila, A. F.; & Galal, A. A. 2022. Controlling the kinematics of a spring-pendulum system using an energy harvesting device. *J. low freq. noise, vibr. active control*. **41** (3), 1234–1257. DOI: 10.1177/14613484221077

How to cite this article:
Wahyuni, S., Rini, N.W., & Saefan, J. (2024). On the dynamics of spring-pendulum system: an overview of configuration space and phase. *Jurnal Natural*, 24(1), 22-27.